Macromolecules **1993,** *26,* 5271–5273

Shear-Induced Morphological Structures in Triblock Copolymers

Faith A. Morrison

Department of Chemical Engineering, Michigan Technological University, Houghton, Michigan 49931-1295

Jimmy W. Mays

Department of Chemistry, University of Alabama, Birmingham, Birmingham, Alabama 35294

M. Muthukumar

Polymer Science and Engineering Department, University of Massachusetts, Amherst, Massachusetts 01003

Alan I. Nakatani* and Charles C. Han

Materials Science and Engineering Laboratory, National Institute of Standards and Technology, Technology Administration, U.S. Department of Commerce, Gaithersburg, Maryland 20899

Received March 22, 1993
Revised Manuscript Received July 19, 1993

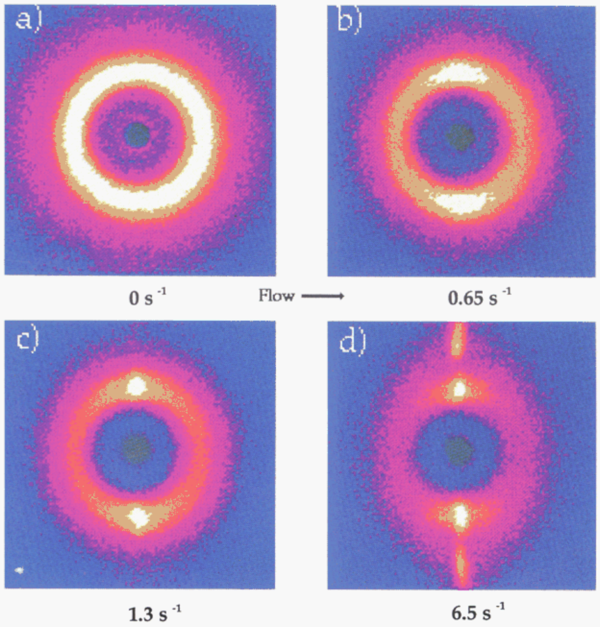

Figure 1. Shear rate dependence of scattering patterns at 116 °C: (a) 0, (b) 0.65, (c) 1.3, (d) 6.5 s^{-1}. The shear direction is horizontal in all scattering patterns shown.

Although there have been numerous experimental and theoretical studies on the variation of block copolymer microstructure with composition and temperature, there have been relatively few studies on the effects of shear on block copolymer morphology. Hadziioannou et al.[1] and Morrison et al.[2,3] examined the effect of steady shear on the structure of triblock copolymers by various techniques such as small-angle X-ray scattering (SAXS), transmission electron microscopy (TEM), and dynamic mechanical measurements. For triblock copolymers with a composition which forms a cylindrical morphology below the order–disorder transition (ODT) temperature, the cylinders were observed to orient along the flow direction upon shearing, with no change in the cylinder radius. In an attempt to produce monodomains of cylindrical morphology in triblock copolymers, Albalak and Thomas[4] have used a novel roll-casting technique that produced cylinders which are slightly thinner and more closely spaced than in the case of solvent-cast films. Bates and co-workers[5,6] have examined the effects of oscillatory shear on diblock copolymers by small-angle neutron scattering (SANS) and dynamic mechanical measurements. For materials with an equilibrium lamellar morphology, application of oscillatory shear at temperatures below the ODT produced two different phases: a perforated lamellar phase and an undefined bicontinuous phase. In all cases cited above, the morphological measurements have been made on quenched samples.

We report on the morphology of a styrene–butadiene–styrene triblock copolymer (23 wt % styrene, cylindrical morphology) in a steady shear field as determined by SANS. The triblock copolymer was examined as a function of temperature and shear rate above and below the ODT. For certain temperatures and shear rates, the scattering behavior on cessation of shear was also measured as a function of time. Using a couette geometry shear cell which allows for in-situ determination of the SANS behavior as a function of temperature and shear rate, possible artifacts due to quenching have been eliminated. We have found evidence for a new shear-induced morphological state.

Living diblock copolymer was produced by sequential polymerization of styrene-d_8 and 1,3-butadiene using *sec*-butyllithium as initiator and benzene as solvent. The precursor polystyrene block has $M_w = 8 \times 10^3$ and $M_w/M_n = 1.03$ as determined by size-exclusion chromatography (SEC). Triblock was produced by coupling the living diblock under vacuum using dichloromethylsilane, followed by fractionation to remove residual diblock polymer. The overall architecture of the triblock is $8 \times 10^3/54 \times 10^3/8 \times 10^3$ ($M_w/M_n = 1.05$). NMR analysis of the polydiene microstructure indicated ca. 50% trans-1,2, 40% cis-1,4, and 10% 1,2 units as anticipated based upon polymerization conditions. The ordered phase of this sample has a hexagonally packed cylindrical morphology, and the ODT determined by dynamic mechanical measurements is 116 °C.

A detailed description of the SANS shear cell has been given previously.[7] The shear gradient is oriented so that the incident beam is parallel to the gradient axis (y-direction), and scattering is monitored in the x–z plane (x is the flow direction and z is the vorticity axis). The SANS experiments were performed at the Cold Neutron Research Facility (CNRF) at the National Institute of Standards and Technology (NIST) using an incident wavelength of 0.9 nm. The data were collected over a two-dimensional detector parallel to the x–z plane and were corrected for background scattering and the empty cell scattering. Intensity calibration was performed using a silica gel as a secondary standard.

In Figure 1, the two-dimensional SANS profiles are shown as a function of shear rate (0, 0.65, 1.3, and 6.5 s^{-1}) at 116 °C. At zero shear, an isotropic peak is observed ($q_{\max} = 0.29 \pm 0.01$ nm^{-1}, $\theta = 2.4 \pm 0.1°$, where $q = (4\pi/\lambda)\sin(\theta/2)$, λ is the incident wavelength, and θ is the scattering angle), which corresponds to a powder pattern from a rod-shaped microstructure with randomly oriented grains. With the application of shear (Figure 1b,c), the scattering becomes anisotropic, with peaks ($q_{\max 1} = 0.29 \pm 0.01$ nm^{-1}, $\theta = 2.4 \pm 0.1°$) appearing normal to the flow direction indicative of the cylinders aligning along the flow direction. Beyond a critical shear rate (Figure 1d), the peaks become narrower azimuthally, reflecting the increasing orientation of the grains, and a second set of peaks appears at higher q ($q_{\max 2} = 0.50 \pm 0.01$ nm^{-1}, $\theta = 4.1 \pm 0.1°$). The ratio of q values for the two sets of peaks is 1:1.7. Although this ratio is consistent with reflections from the 100 and 110 planes in a hexagonally packed cylindrical array with unit cell parameter $a = 25 \pm 0.5$ nm, the data taken after

0024-9297/93/2226-5271$04.00/0

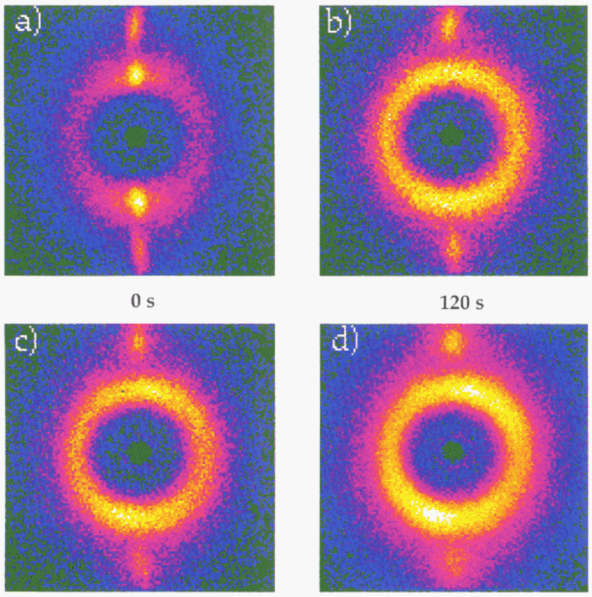

0 s

120 s

360 s

1200 s

Figure 2. Time dependence of scattering patterns after cessation of shear (6.5 s^{-1}) at 116 °C: (a) 0 s, (b) 120 s after shear, (c) 360 s after shear, (d) 1200 s after shear.

cessation of shear show that a more detailed analysis of the origins of the second peak is required.

In Figure 2, the time dependence of the scattering behavior (0, 120, 360, and 1200 s) after cessation of shear (6.5 s^{-1}) is shown at 116 °C. After cessation of shear, the lower q peaks broaden azimuthally as a function of time, while the higher q peaks remain sharp. This is the first evidence that the two peaks arise from two distinctly different types of oriented grains in the sheared specimens. When the time evolution of the two sets of peaks with an applied shear rate is examined, the relative intensities of the two peaks change. This also strongly suggests that the higher q peak is unrelated to the lower q peak.

From the evidence in Figure 2, we believe that the second, high q peak results from a new structure. This structure is distinct from the original structure which only gives rise to the low q peak. Below the ODT in the quiescent state, the triblock copolymer exists in a hexagonally packed array of cylinders ($a = 25$ nm), with the polystyrene blocks residing in the cylinders and the polybutadiene blocks in the matrix. There is a proliferation of grains of such morphology with uncorrelated orientations of the grains. In our model of the microstructure under shear, the original grains of hexagonally packed cylinders ($a = 25$ nm) align with the flow (Figure 3a). These grains are randomized in a cylindrically symmetric fashion about the flow axis. This is consistent with earlier reports on quenched samples of similar triblock systems prepared at comparatively low shear rates.[2] Above a critical shear rate, however, a new structure forms which preserves some grains of the low shear structure. Simultaneously, through the reorganization and transformation of other grains, new grains of a different structure are created. Therefore, we propose that, at high shear rates, the sample consists of two types of grains: the first type of grain remains the invariant with shear, while the second grain structure has one of the two hypothesized forms outlined below.

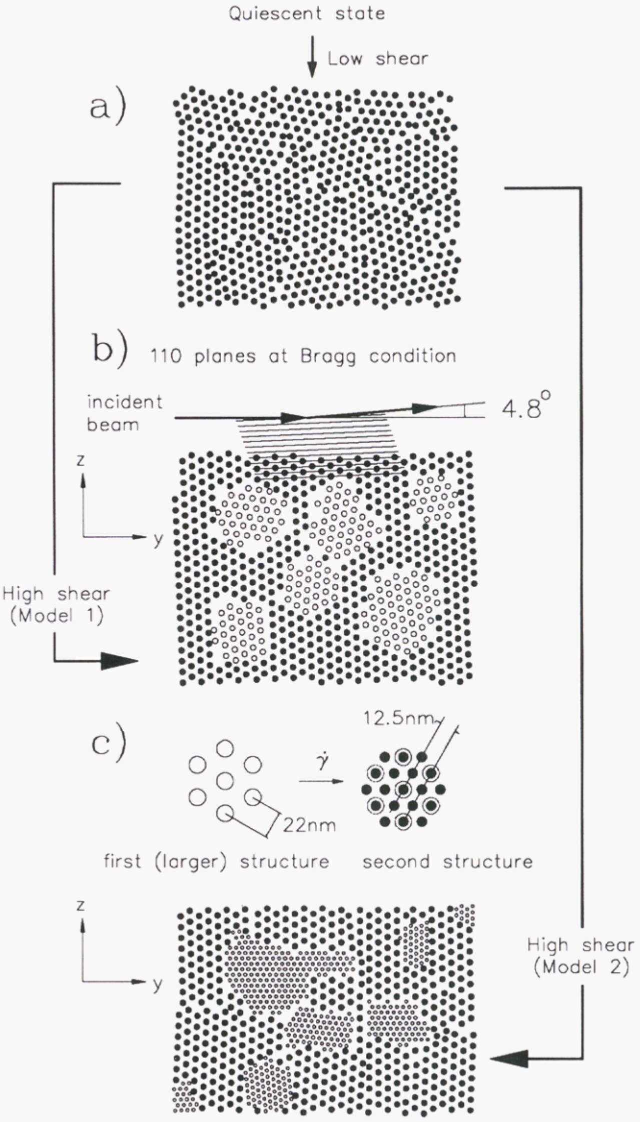

Figure 3. Schematic drawings: (a) Low shear structure showing grains of random rotational orientation and all cylinder axes parallel to flow. (b) Model 1, showing hexagonally packed cylinders with near perfect order and randomly oriented grains of cylinders. Dark circles depict shear-induced PS morphology. (c) Model 2, showing two types of grains containing hexagonally packed cylinders with different lattice spacings. Open circles depict shear-induced polystyrene morphology. The inset shows the relation between the large and small lattice structures. Grain sizes shown in these figures may not necessarily reflect the true grain sizes.

In the first hypothetical model, the second "grain" structure consists of the cylinders in a nearly perfect, hexagonally packed, continuous domain. We assume that the 110 Bragg planes of the continuous domain are approximately oriented at an angle of 2° (half of $2\theta = 4.1°$) relative to the $x-y$ plane. With the incident neutron beam parallel to the y-axis, this orientation of the 110 planes satisfies the Bragg condition, giving rise to the high q peak ($d_{110} = 12.5 \pm 0.5$ nm). At this stage, we cannot justify this preferred orientation of the 110 Bragg planes except for the fact that the scattering data are consistent with such an orientation. Hadziiouannou et al. also observed a unique orientation of aligned cylinders relative to the flow direction.[1] Within this continuous domain, grains containing cylinders of the same unit cell spacing remain. Apart from a preferred orientation of the cylinders parallel to the flow direction, the orientations of these grains are not correlated nor are they correlated with the continuous phase (Figure 3b). The random rotational orientation of the grains about the c-axis of the unit cell (the c-axis is oriented parallel to the flow direction) allows the 100 Bragg planes of certain grains to satisfy the Bragg condition ($d_{100} = 22 \pm 0.5$ nm), giving rise to the low q peak. Since the continuous structure forms at the expense of the grains, the ratios of the peak intensities vary as a function of shear rate, as would be expected. The grains with a distribution of orientations also relax faster after cessation of shear, which would account for the independent azimuthal broadening of the low q peak.

In the second hypothetical model, two types of grains exist, consisting of two hexagonally packed, cylindrical arrays with different unit cell dimensions. We suppose that, above the threshold shear rate, chains in a bridging configuration between cylinders may be subject to an additional stretching in the flow direction, causing polystyrene blocks to disengage from the cylinders. The cylinders then reassemble, with the chains in a predominantly looping configuration (polystyrene blocks of a chain reside in the same cylinder), to form a hexagonal array giving the second grain structure. In this second structure, the cylinders are thinner and closer to one another in comparison with the first structure (Figure 3c). The spacing of cylinders ($d_{100} = 12.5 \pm 0.5$ nm, $a = 14$ nm) in the closely packed grains corresponds to the second scattering peak. At a given temperature and shear rate, the system may be considered to be a polydomain, where some of the grains are made up of the first structure and the remaining grains are made up of the second structure. The propensity, size, and continuity of the grains of the second type are determined by the shear rate and temperature for a given triblock polymer. With cessation of shear, the orientation of the more closely packed second structure must relax much more slowly to account for the data in Figure 2.

The models proposed here account for all the essential features of the scattering data but are by no means exclusive and may need to be modified as more experimental evidence is gathered. The two proposed states cannot be distinguished from our current data. However, the evidence indicates that distinct morphological states exist. SANS experiments in the y–z plane and TEM studies are currently in progress in order to differentiate between the two models. More detailed issues related to chain configurations, different time scales, surface effects, sample orientation, grain boundaries, and modification of the phase diagram for triblock copolymers by shear will be addressed in a future publication.

Acknowledgment. The authors acknowledge Drs. F. A. Khoury, E. A. Di Marzio, and C. L. Jackson for many enlightening discussions concerning this work. F.A.M. acknowledges the Petroleum Research Fund, administered by the American Chemical Society, and the National Science Foundation (Grant DMR 9111318) for partial support of this research.

References and Notes

(1) Hadziioannou, G.; Mathis, A.; Skoulis, A. *Colloid Polym. Sci.* **1979**, *257*, 15.

(2) Morrison, F. A.; Winter, H. H. *Macromolecules* **1989**, *22*, 3533.

(3) Morrison, F. A.; Winter, H. H. Gronski, W.; Barnes, J. D. *Macromolecules* **1990**, *23*, 4200.

(4) Albalak, R. J.; Thomas, E. L. *J. Polym. Sci., Part B: Polym. Phys.* **1993**, *31*, 37.

(5) Almdal, K.; Koppi, K. A.; Bates, F. S.; Mortensen, K. *Macromolecules* **1992**, *25*, 1743.

(6) Bates, F. S.; Rosedale, J. H.; Fredrickson, G. H. *J. Chem. Phys.* **1990**, *92*, 6255.

(7) Nakatani, A. I.; Kim, H.; Han, C. C. *J. Res. Natl. Inst. Stand. Technol.* **1990**, *95*, 7.